

Design Configurations of Focusing Lenses for PXIE SSR1 Cryomodule

I. Terechkine

I. Introduction

Functional and technical requirements for focusing lenses in the SSR1 cryomodule of PXIE test facility were modified several times reflecting the progress in understanding beam dynamics, content of commissioning tests with and without particle beam in the cryomodule, and technical complexity associated with implementation of some of the requirements. The first set of requirements for lenses in the SSR1 cryomodule was placed in the PXIE document base on Dec. 17, 2011 as part of the SSR1 cryomodule functional specification [1] and postulated 6.2 T²m focusing strength of the lens, 0.02 T-m bending strength of the steering dipoles, ± 0.2 mm maximum allowed deviation of the magnetic axis of the lens from the theoretical beam trajectory (200 mm reference base), and 100 G fringe magnetic field on walls of superconducting cavities in the cryomodule.

Having in mind the strict alignment precision requirements, and taking into account existing experience in alignment of the HINS linac focusing lenses [2], avoiding mechanical connection between the lens and the beam pipe seemed a logical step to make.

On the other hand, beam studies at the commissioning stage involve using a beam position monitor (BPM), which is convenient to have attached to focusing lenses, as its position is well controlled. In this case, focusing lenses of the cryomodule must incorporate part of the beam line, and mechanical connection between the lens and SRF cavities cannot be avoided.

Allowed level of magnetic field on walls of superconducting cavities was subject of multiple discussions. Although environmental magnetic field (that is the field which is present in the cryomodule during cooling down) must be on the level of several micro-Tesla in accordance with [3], known practice of using magnets inside cryomodules proves that the magnetic field on cavity walls associated with these devices can be much higher [4]. Practical limit to the level of this field is set by possible quenches in SRF cavities that can result in degradation of cavity performance after quenching, so the magnetic field generated by magnetic elements inside cryomodules must be sufficiently small to limit the degradation. Before dynamics of the magnetic flux trapping in walls of superconducting cavities was studied (e.g. see [5]), the maximum value of the magnetic field on cavity walls was reduced from 100 G to a more conservative value of ~ 10 G [6], and it became necessary to find a way to reduce the fringe magnetic field of focusing lenses at least to this level.

Although employing materials with ferro-magnetic properties as main flux returns of focusing solenoids (e.g. see [7]) can significantly simplify lens design, these materials can potentially be magnetized and generate magnetic field before the system is cooled down, which can result in the cavity quality factor degradation. If a design with a passive (ferromagnetic) flux return is considered, the magnetization issue must be studied to understand what design measures

are needed to solve the problem. It is possible though to bypass the magnetization problem by using the active shielding lens design.

The final set of the requirements [8] was developed as a result of several iterations in the beam optics and the cryomodule design studies and postulates $4.0 \text{ T}^2 \cdot \text{m}$ integrated squared field strength, $0.0025 \text{ T} \cdot \text{m}$ steering dipole strength, and $\pm 0.2 \text{ mm}$ RMS alignment accuracy for a 200 mm base distance. Significantly relaxed requirement for the alignment precision, although still tight, is now within the accuracy range of optical measurement devices, like contemporary laser tracker. A 2K coolant temperature, 100 A maximum current in the lens, and 30-mm minimum beam bore diameter are other important parameters needed to start the lens design study.

This note provides basic information and relevant details of three main approaches to the SSR1 focusing lens design:

- Lens with passive shielding is mechanically separated from the beam pipe,
- Lens with passive shielding is integrated with the beam pipe (both employing a LHe vessel and conductively cooled),
- Lens employs active shielding.

For the first two cases, studies of residual magnetization in ferromagnetic shielding have been made.

The note does not contain a solution for the lens design; it provides information needed to generate a decision on a design approach to follow. A decision making process will take into account not only engineering data presented in this note, but also other information, including (but to restricted to) the type of the lenses used in other cryomodules of PXIE and fabrication abilities of a potential vendor.

II. Evaluation of the level of magnetic field on the SSR1 cavity walls

Simple evaluation of magnetic field generated by a focusing lens can be made by employing a concept of effective magnetic moment, that is the product of the ampere-turns Iw in a loop with the radius a and the cross-section of the loop $S = \pi a^2$. The magnetic field on the axis z can be expressed as

$$B_z = 2 \cdot \mu_0 \cdot Iw \cdot S / (a^2 + z^2)^{3/2}$$

Taking the integral of $(B_z)^2$ over the length along the axis (that is from $-\infty$ to $+\infty$) and demanding this integral be equal to the required focusing strength FS of the lens results in the requirement to have the total current in the loop

$$(Iw)^2 = 2 / (3 \cdot \pi^3 \cdot \mu_0^2) \cdot a \cdot FS$$

With the loop radius $a = 25 \text{ mm}$, this results in the requirement to have $Iw \approx 36,000$ or the magnetic moment $Iw \cdot S \approx 75 \text{ A} \cdot \text{m}^2$. Using this number in the expression for the magnetic field at the distance of $\sim 0.25 \text{ m}$ from the loop center, we get evaluation of the magnetic field on the walls of the cavity if no measures are taken to shield this field: $B_{0.25\text{m}} \approx 0.012 \text{ T}$ or 120 G . This is about one order of magnitude higher than the fringe field requirement; so shielding the cavity from this field seems necessary. Let's consider the systems with passive shielding first.

III. Focusing lens is not mechanically connected to the beam pipe; passive shielding

As was mentioned earlier, it is possible to significantly improve reproducibility of the lens position in a cryomodule after thermo-cycling by mechanically separating a focusing lens from the beam pipe. To check on feasibility of this design approach, and assuming 2K temperature of the winding, 6.2 T²·m focusing strength was set as a goal for this case study. To make lens design as simple as possible, the next design measures were considered:

1. No bucking coils, as in [7], are employed. A one-coil system with does not require any measures to constrain repulsion of coils in the lens.
2. A passive (ferromagnetic) flux return is used to restrict spatial extent of the magnetic flux in the cryomodule; the flux return is located outside the LHe vessel of the lens; this makes the LHe vessel very compact.
3. Layers of shielding made of permalloy-type material are used to bring the magnetic field on the SSR1 cavity walls to the desired level.
4. Steering coil assembly is placed inside the lens, as it was made in [7].

Fig. 1 shows the lens design concept.

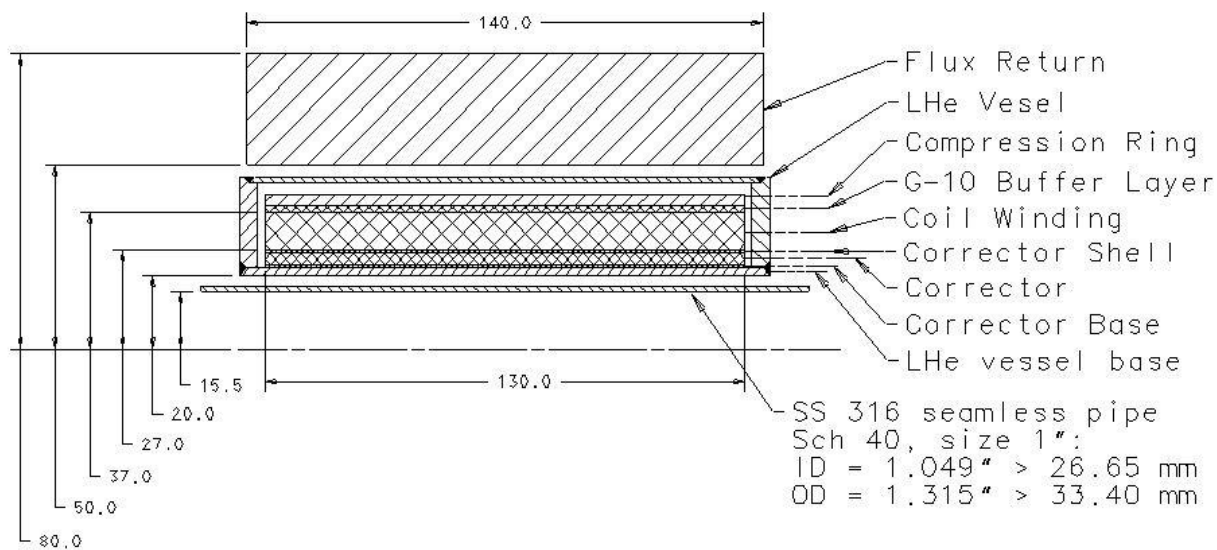


Fig. 1. Single-coil design with flux return outside LHe vessel.

The lens is assembled around the beam pipe and is not mechanically connected to it. Dipole corrector assembly is fabricated independently; the technique of the corrector fabrication is well established and described elsewhere (see [7] for further reference). The coil is wound on a stainless steel spool using NbTi strand. Table 1 provides comparison of the specified critical current of a 0.5 mm strand made by OXFORD Instr, Inc. at 4.2 K with results of measurements of several samples and with what is calculated using a parameterized expression for the critical current density in [9] at 4.2 K. Using parameterized expression for the critical current density allows extrapolation of the existing data for the round 0.5 mm strand at 4.2 K to any strand size

at any temperature. As 0.4 mm strand was chosen for this design, the table also compares the specified critical current with what the parameterized expression gives at 4.2 K.

Table 1. Specified, measured, and calculated critical current of 0.5 mm strand at 4.2 K

	B (T)	8	7	6	5	4	3	2	1
Specified - 0.5 mm	Ic (A)	94	134	173	213	252			
Sample1 - 0.5 mm	Ic (A)	98	151	202	255	308	367	451	621
Sample2 - 0.5 mm	Ic (A)		154	206	258	310	370	456	646
Modeling - 0.5 mm	Ic (A)		126		207				
Specified - 0.4 mm	Ic (A)		86	113	140	167	194		
Modeling - 0.4 mm	Ic (A)		81	108	134	164			

The flux return of the lens is made of low-carbon steel, and the magnetic shield is made of electric grade steels and/or permalloy-type material. Details of the shield geometry can be adjusted for a better fit inside the cryomodule. Fig. 2 shows two, quite different ways of making this shield (only one quarter of the lens is shown). Both designs employ a thin permalloy sheet installed perpendicular to the beam pipe in the vicinity of SFR cavity, although other locations of this sheet were also successfully tried; both designs provide the needed degree of shielding.

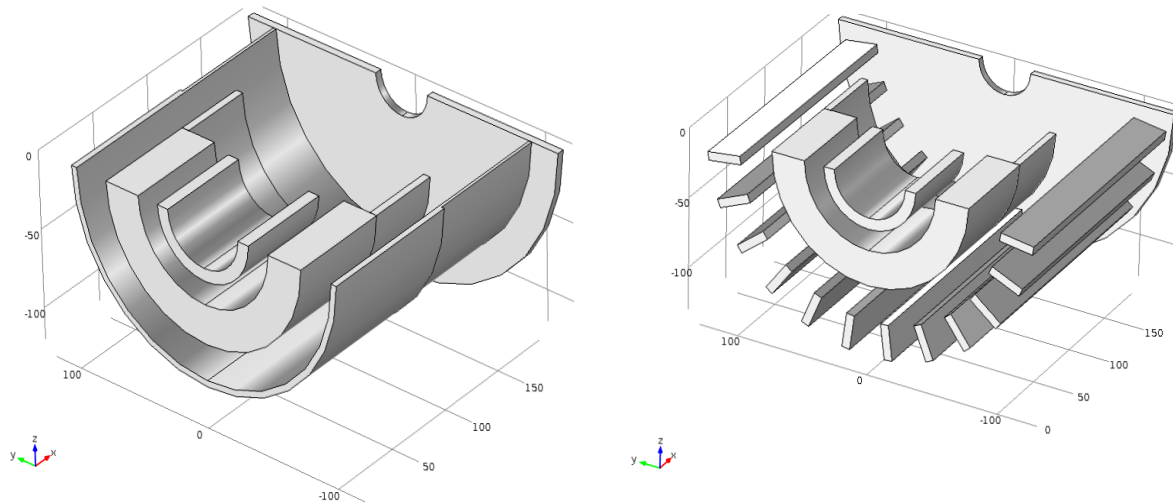


Fig. 2. Configurations of the secondary magnetic shield

The flux return part of the magnetic shield can be made of electric grade steel, silicon grade steel, or permalloy-type material. A map of fringe magnetic field and a graph of the field in the plane $Z = 250$ mm (where the nearest cavity wall is located) is shown in Fig. 3 for the case of the “squirrel wheel” shield flux return design and $4 \text{ T}^2\text{-m}$ strength of the lens; magnetic field is less than ~ 4 G on the cavity wall. Magnetic elements of the lens are far from being saturated; this provides an opportunity to leave big gaps between the rods of the “squirrel wheel” flux return and leaves plenty of space for mechanical features needed to mount and align the lens (Fig. 4).

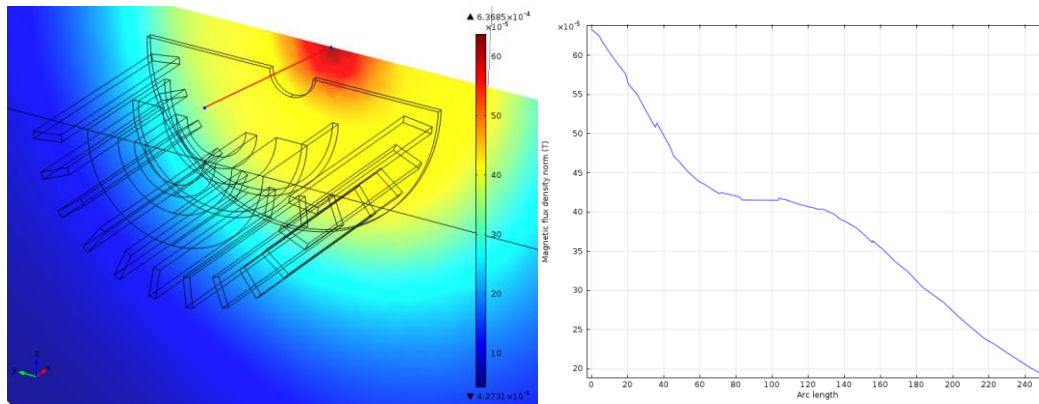


Fig. 3. Fringe field map for the lens with $4.0 \text{ T}^2\text{m}$ focusing strength.

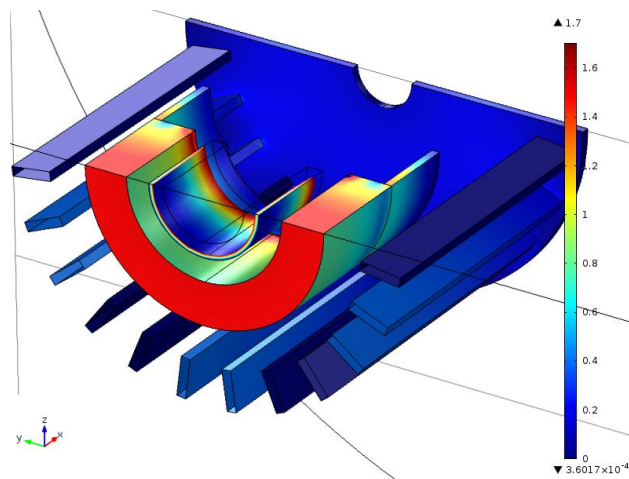


Fig. 4. Flux density in the magnetic elements of the lens with the focusing strength of $4 \text{ T}^2\text{m}$

Main parameters of this lens can be found in the list below.

Solenoid :

$R_i = 27 \text{ mm}$, $R_o = 37 \text{ mm}$, $L = 130 \text{ mm}$,

Oxford $54 \times 6 \times 0.4 \text{ mm}$ strand, $N = 6535$

Winding density factor is 0.65

Coolant temperature – 2 K

$I_{cr} = 133 \text{ A}$

$B_{cr} = 7.7 \text{ T}$

$\int B^2 dl = 6.6 \text{ T}^2\cdot\text{m}$ at maximum current, with the flux return.

Primary flux return:

$R_i = 50 \text{ mm}$, $R_o = 80 \text{ mm}$, $L = 140 \text{ mm}$

50 mm long, 5 mm thick flux catchers are optional and help to reduce the fringe field.

Cryoperm10 shielding:

Thickness – 2 mm, longitudinal position – 185 mm, outer radius – 135 mm

Secondary flux return:

Number of bars– 12, cross-section – $26 \times 6 \text{ mm}^2$, radial position of the inner side - 105 mm

Fig. 5 provides a layout of the lens in the SSR1 cryomodule.

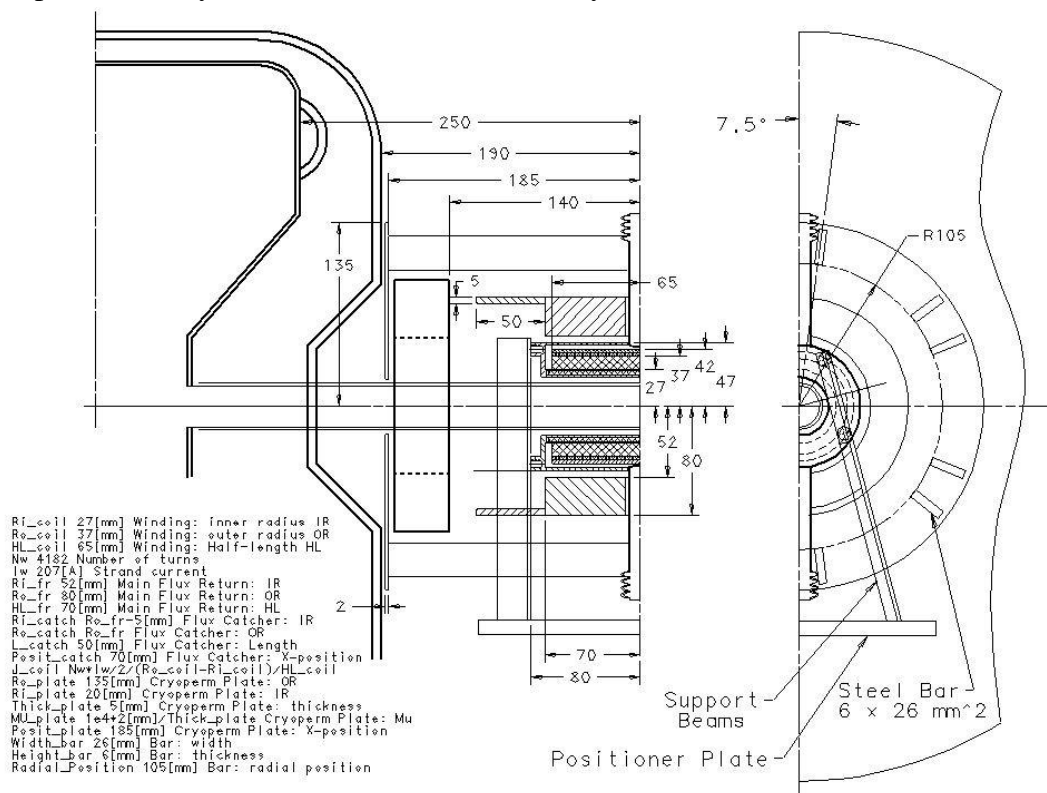


Fig. 5. Layout of the lens in the SSR1 cryomodule

In this configuration, the transverse (Cryoperm-10) plate of the secondary shield is located between the beam of the cavity tuner and the vacuum vessel of the cavity. There is considerable freedom in further optimization of this configuration, including different secondary flux return design and different position of the Cryoperm10 plate. Because in this example the flux return is located outside the LHe vessel, it can be built of several pieces, which can simplify the assembly. The LHe vessel can be quite compact, containing small amount of LHe. As a result small diameter piping can be used to connect the vessel to the phase separator, which helps to reduce undesirable forces applied to the lens assembly.

IV. Focusing lens is mechanically connected to the beam pipe; passive shielding

During linac commissioning stage, it is often found convenient to have beam position monitors attached to focusing lenses inside cryomodules. In this case, the beam pipe needs to be integrated in the focusing lens. This approach requires using two bellows in the beam line to make possible adjustment of the lens position. To some advantage of this approach, the coil diameter can be a bit smaller, which results in smaller magnetic flux, which simplifies the shielding. Two options will be studied here. The first option will explore using a 2 K coolant temperature to make the coil as small as possible, and the second option will study a conduction cooling approach, which cannot guarantee the 2 K temperature of the winding.

A. Lens winding is in a bath of LHe at 2K

For this case, it was straightforward to find a design solution based on what was done for the much more demanding case analyzed in the previous chapter. The next set of the lens parameters was chosen: $R_i = 22.5\text{ mm}$, $R_o = 29\text{ mm}$, and $L = 112.5\text{ mm}$, the coil is wound using 0.4 mm NbTi strand; compaction factor is 0.65 and the total number of turns $N = 3797$. Maximum current (at quench) is 168 A , $B_{cr} = 6.6\text{ T}$. Although the current is higher than was requested by the specification, it can be reduced as needed by choosing a finer strand.

If no flux return is used, the field on the wall of the cavity at $Z = 250\text{ mm}$ reaches $\sim 120\text{ G}$, which is consistent with what was evaluated in section II. If a 150 mm long, 25 mm thick flux return is added with $R_i = 31\text{ mm}$, the maximum field on the nearest wall is $\sim 30\text{ G}$. Adding a single layer magnetic shield made of Cryoperm-10 brings the fringe field to the desired (low) level of less than 3.5 G . Integrated strength of the lens with the flux return is $4.56\text{ T}^2\text{m}$.

In this case, an attempt was also made to investigate a possibility of using low-carbon steel flux return as a compression ring of the coil assembly; this implies that LHe vessel needs to contain not only the coil, but also the flux return; nevertheless the outer diameter of the LHe vessel is still quite small: $\sim 120\text{ mm}$.

Fig. 6 shows the magnetic field in the flux return and in the secondary shield and a graph of the field in the plane $Z = 250\text{ mm}$. The field on the wall is well within the specified 10 G limit.

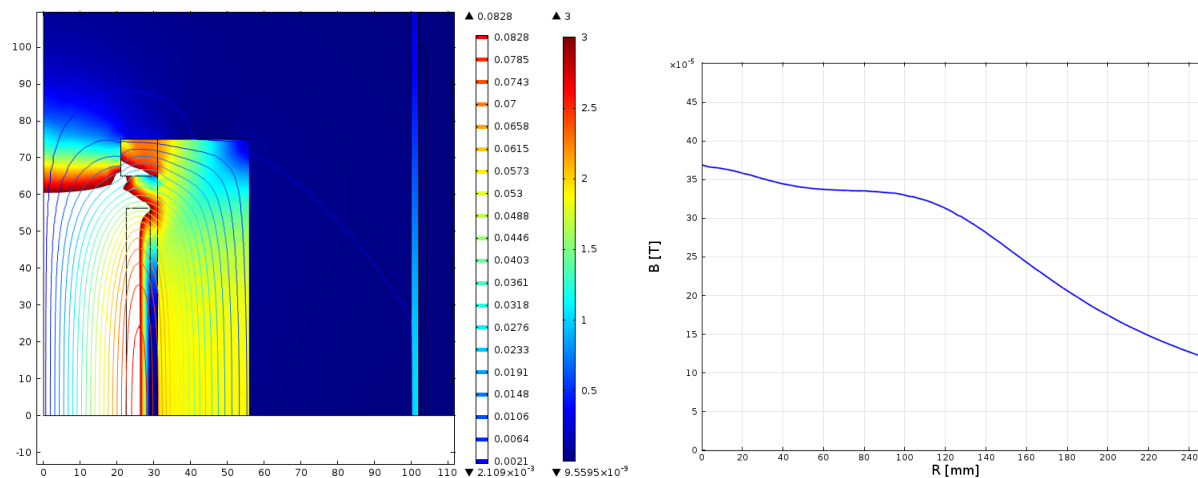


Fig. 6. 2 K version of the SSR1 lens

To simplify alignment process, it would be convenient to rely on geometric features of focusing lens assembly; in this case, position of the magnetic and geometric axis of the lens must be well correlated. The existence of a LHe vessel significantly complicates the task of alignment based on the position of the geometric axis as no direct access is available to the inner bore of the lens and to features hidden inside the LHe vessel. Using intermediate fiducials for the alignment inevitably results in some loss of the accuracy. Alignment precision can be improved if parts of the lens can be mechanically accessible. One of the ways to provide this access is to use conduction cooling, where cooling pipes are attached to a low-carbon flux return that is used as a compression ring and is not hidden in a LHe vessel.

B. Lens winding is conductively cooled

One of possible schemes to design a conductively-cooled lens is shown in Fig. 7.

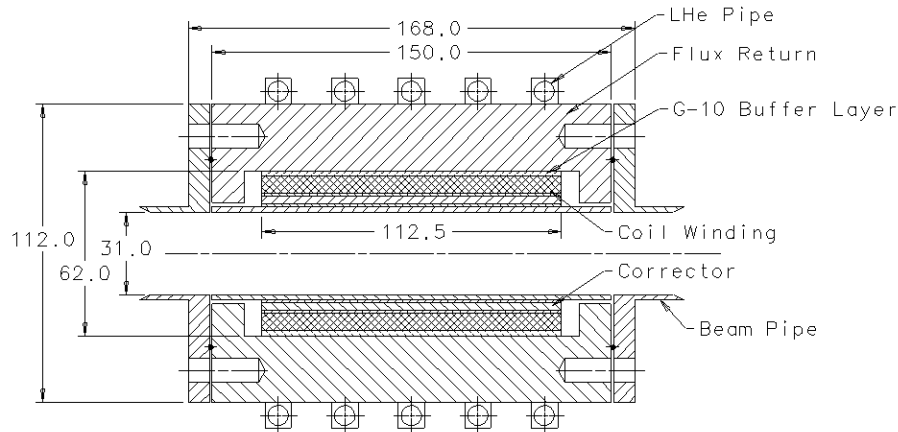


Fig. 7. 2.5 K version of a conduction-cooled lens

Because of good thermal conductivity of low carbon steel at low temperatures, this cooling scheme can be a decent choice, especially if to consider the openness of all surfaces for use during the alignment process. On the other hand, this openness results in somewhat elevated temperature of the winding due to parasitic heat flux that reaches the surface of the lens. With some reservations, we can count on the winding temperature being below 2.5 K [10]. The increased temperature of the superconductor leads to lower maximum current density and fatter coil. The goal of this exercise was to verify that the fringe field requirement still can be met.

One of possible design solutions can be as the following:

$R_i = 22.5$ mm, $R_o = 29$ mm $L = 112.5$ mm. As earlier, a 0.4 mm NbTi strand was used, and winding was made with the compaction factor of 0.65; the total number of turns $N = 4055$. The secondary shielding is made similar to what was tried earlier, and there were no problems in meeting the fringe field requirement.

The maximum current at quench is 160.2 A, with $B_{cr} = 6.7$ T. The focusing strength of the lens with the flux return is 4.5 T²m. Fig. 8 shows the layout of this version with the field map in the flux return and in the secondary shield and a graph of the field in the plane $Z = 250$ mm.

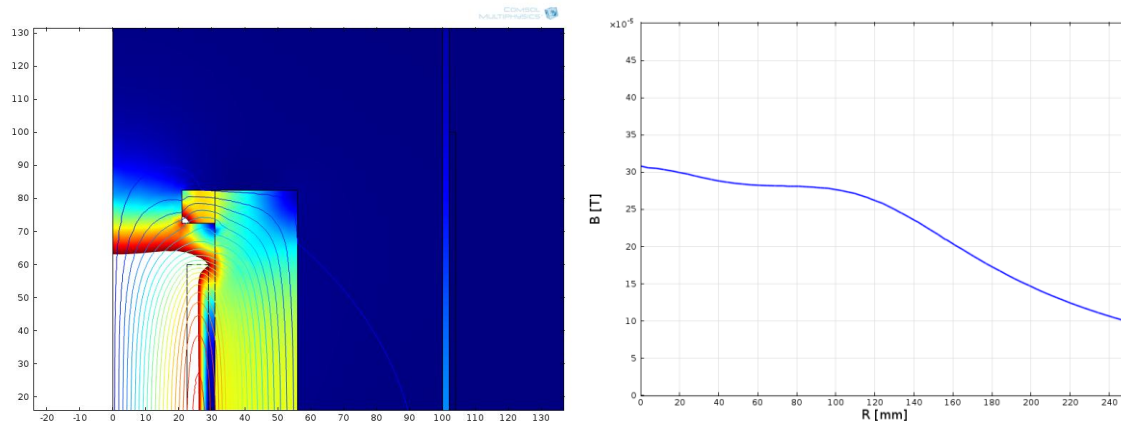


Fig. 8. 2.5 K version of the SSR1 lens

Maximum magnetic flux density in the central part of the flux return is ~ 1.85 T. In the magnetic shield, the field is ~ 0.9 T in the central part made of one 2-mm thick sheet of electric grade steel and ~ 0.1 T in the end pieces made of Cryoperm-10.

As was mentioned earlier, using magnetic materials in the flux return and in the magnetic shield inevitably results in a residual magnetization of these materials, which will not disappear when the system is warmed up unless demagnetization is made. As RF cavities are warmed up, the residual magnetic field penetrates their walls, which results in the quality factor drop after cooling down and increased power loss. Demagnetization procedure, although proved to be effective, will increase of the downtime of the system during inevitable thermal cycling.

In the following chapter, residual magnetization in parts of a passively shielded focusing lens will be analyzed and corresponding means of protection will be suggested.

V. Residual magnetization of the flux return and the magnetic shield

The purpose of using a flux return made of a ferromagnetic material is to effectively shunt the free space, so that the magnetic flux generated by the coils in the lens is spatially restricted. To reduce the size of a flux return, it is essential to choose material with high saturation flux density, like soft steel with the saturation flux density reaching 2 T. Other parameters to take into account are residual flux density B_R and coercive force H_c ; these two parameters define magnetic field and the flux density remaining in the material after the magnetizing force is removed. Coercive force of soft steels strongly depends on its chemical content and heat treatment regimen, which changes the grain size. Best electric grade steels have coercive force ~ 50 A/m (or ~ 0.5 Oe). For example, data from LTV Steel Company show that low-carbon steel ($< 0.005\%$ C) with low nitrogen content ($< 0.005\%$ N) after additional stress-relief annealing, and after being magnetized to ~ 2 T, has $B_R = 1.3$ T and $H_c = 0.6$ Oe (SMS-3 steel). Electric grades of silicon steels have $H_c \sim 40$ A/m, and $B_R \sim 1$ T with the saturation flux density $B_s \approx 2$ T. Structural grades of soft steel (e.g. 1008 – 1012) have coercive force higher than 80 A/m; annealing in hydrogen can be used though to lower the coercive force. Relatively high coercive force of steels results in noticeable residual magnetization that can generate unwanted magnetic field in the vicinity of RF cavities.

To effectively shield the magnetic field and reduce remnants, materials with low coercive force must be employed; often Ni-Fe alloys (or permalloys) are used for this purpose. Permalloy containing 78% of Ni has the coercive force $H_c = 4$ A/m, and the coercive force of Supermalloys can be as low as 0.5 A/m. Permeability of these materials reaches and exceeds 10^5 , and they are widely used as shielding materials. On the left side of the magnetization curve for permalloys, the slope of the curve can reach 10^6 . Residual flux density of Ni-Fe alloys is ~ 0.5 T. These materials were designed for work at room temperature, and in cryo-environment their properties are significantly weaker.

Cryoperm-10 is a permalloy-type material optimized for work at low temperatures. It has the coercive force $H_c \approx 8$ A/m and permeability reaching and exceeding 10^5 . Another material on the

If only the main flux return is employed and no shielding is in use, the field on the nearest wall of a cavity (at $Z = 250$ mm) reaches ~ 100 G. When a 2-mm thick primary magnetic shield is used, the magnetic field in this part at the maximum current is below 1 T (Fig. 10). Performance of this shield is close to optimal if low carbon steel is used to make its cylindrical part.

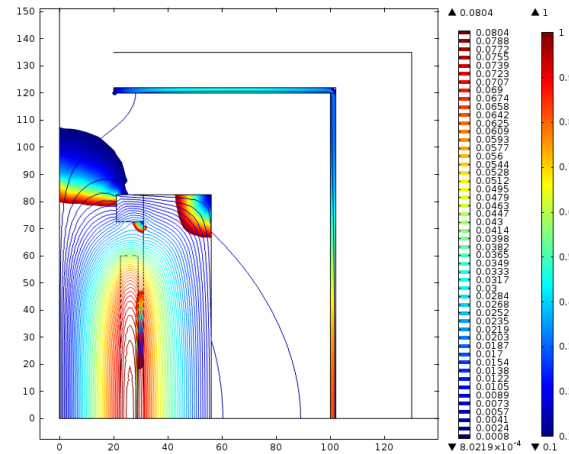


Fig. 10. Magnetic field map in the lens' primary magnetic shield at the maximum current

Even when the “cleaning” (or secondary) shield made of Cryoperm-10 is not used, the fringe magnetic field is below the specified 10 G level. The first graph in Fig. 11 shows the magnetic field along the radial (front) wall, and the second graph is plotted along the outer cylinder starting at $Z = 250$ mm towards the median plane of the cavity at $Z = 400$ mm. The secondary magnetic shield is not needed to reach the specified level of the fringe field, it is needed only to provide protection against the residual magnetization.

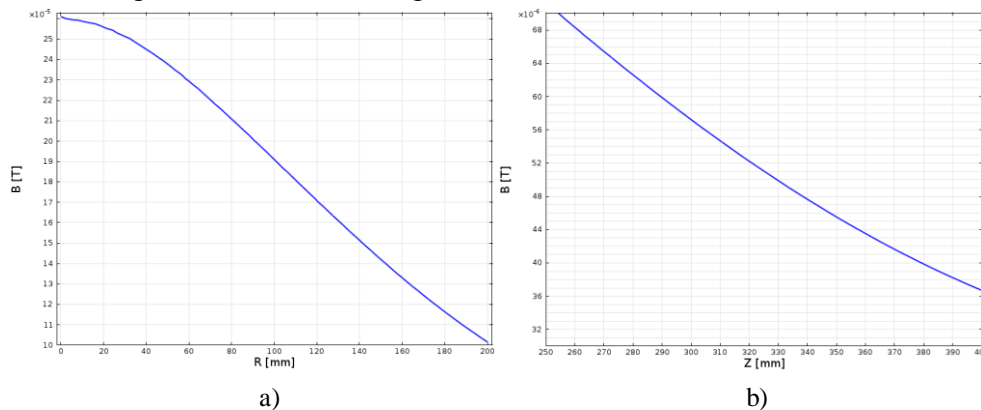


Fig. 11. Magnetic field on the cavity walls when only the primary magnetic shields is used: along the line $Z = 250$ mm (a) and along the line $R = 253$ mm (b)

Fig. 12 shows the magnetic field along the walls of the superconducting SSR1 cavity at maximum current when both the primary and the secondary magnetic shields are activated. Both graphs are built for the case with the permeability of the secondary (cleaning) magnetic shield of 10,000 (it is higher for real material). The field on the walls of the cavity changes from ~ 15 μ T at $R = 90$ mm, to ~ 6 μ T at $R = 200$ mm, to ~ 3 μ T at $R = 253$ mm.

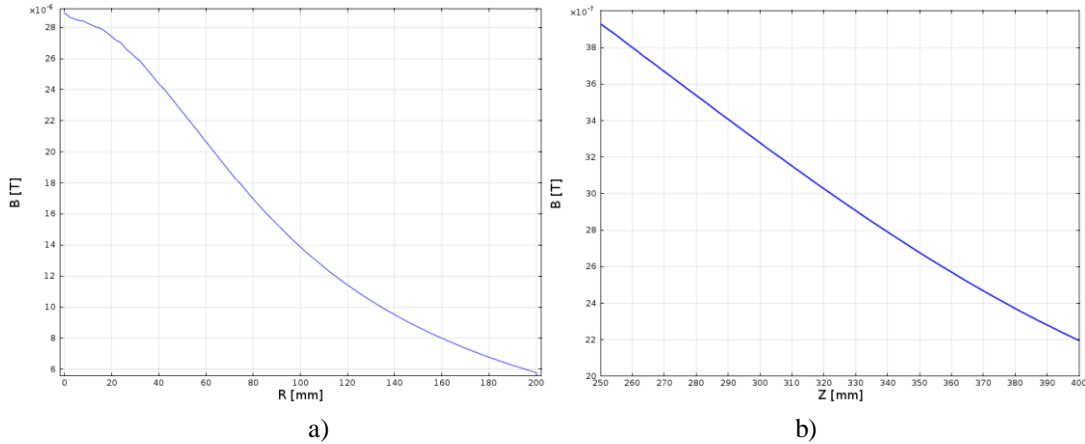


Fig. 12. Magnetic field on the cavity walls when two magnetic shields are used: along the line $Z = 250$ mm (a) and along the line $R = 253$ mm (b)

Till this point, no magnetization of the shield materials was involved. We can study the impact of magnetization by introducing the next substitutive relation between the flux density and the magnetic field:

$$\mathbf{B} = \mathbf{B}_R + \mu_{\text{eff}} \mu_0 \cdot \mathbf{H},$$

where μ_{eff} refers to the slope on the left side of the magnetization curve:

$$\mu_{\text{eff}} \mu_0 = \mathbf{B}_R / \mathbf{H}_C.$$

We will assume $\mu_{\text{eff}} = \text{const}$, which is a good approximation for soft magnetics.

Impact of flux return magnetization will be studied first. By fixing properties of the material used to make shield and varying μ_{eff} of the flux return material, we can extract information about the desired magnetic properties of the flux return by observing the fringe field distribution on the walls of the cavity due to the residual magnetization. For example, if both magnetic shields are used and $\mu_{\text{eff}} = 20,000$ ($B_R = 1.2$ T, $H_C = 50$ A/m), the magnetic field in the plane $Z = 250$ mm $B_{250} < 8 \cdot 10^{-8}$ T. The maximum field in the primary magnetic shield at $Z = 0$ is ~ 25 Gs. As we lower μ_{eff} , the fringe field must grow; with $\mu_{\text{eff}} = 6,000$ ($B_R = 1.2$ T, $H_C = 2$ Oe), the field in the plane $Z = 250$ mm $B_{250} < 28 \cdot 10^{-8}$ T; the maximum field in the primary shield is 85 Gs. If to make $\mu_{\text{eff}} = 3,000$ ($B_R = 1.2$ T, $H_C = 4$ Oe), the fringe magnetic field along the line $Z = 250$ mm $B_{250} < 56 \cdot 10^{-8}$ T; the field in the primary shield is 170 Gs ($1.7 \cdot 10^{-2}$ T).

As we see, residual magnetization of the flux return made of low-carbon steel is well contained by the two layers of magnetic shielding. Although smaller fringe field level can be obtained when quality electric grade steel is used, using stress-annealed structural grades of low-carbon steel seems acceptable.

As the impact of the flux return material choice is understood and small, we can neglect the residual magnetization of the flux return and only consider magnetization of the primary magnetic shield, which must be definitely made of very soft steel (non-oriented silicon steel, or non-silicon grades of quality steels). Sheet materials are well suited for the purpose. If material for this magnetic shield has $\mu_{\text{eff}} = 20,000$ ($B_R = 1.0$ T, $H_C = 0.5$ Oe), the field along the radial line $Z = 250$ mm $B_{250} < 2.2 \cdot 10^{-6}$ T. The maximum field in the primary shield (at $Z = 0$) is 250 Gs.

If $\mu_{\text{eff}} = 10,000$ ($B_R = 1.0$ T, $H_C = 1.0$ Oe), the field along the line $Z = 250$ mm $B_{250} < 4.4 \cdot 10^{-6}$ T. The maximum field in the primary shield is 500 Gs ($5e-2$ T).

The effect of magnetization of the primary magnetic shield is much bigger than that of the flux return; this is because only the secondary shield exists between the magnetized primary flux return and the cavity wall. Nevertheless, if a requirement for the fringe magnetic field on the walls is below $4 \mu\text{T}$, a material with $H_c \approx 1$ Oe is still an option.

Another feature of the magnetic shield to take into account is the size of a hole for the beam pipe (in Fig. 9, diameter of the hole is 40 mm). Let's do the study using this diameter as parameter and observing the field distribution along the radial line $Z = 250$ mm and along the outer border of the cavity $R = 250$ mm. Results of this study are summarized in Table 2.

Table 2. Magnetic field on cavity walls as a function of the diameter of a central hole

Hole diameter	$Z = 250$ mm, $R = 0$	$Z = 250$ mm, $R = 200$ mm	$R = 250$ mm, $Z = 250$ mm	$R = 250$ mm, $Z = 400$ mm
40 mm	$3.4 \mu\text{T}$	$1.2 \mu\text{T}$	$0.8 \mu\text{T}$	$0.45 \mu\text{T}$
50 mm	$4.0 \mu\text{T}$	$1.2 \mu\text{T}$	$0.87 \mu\text{T}$	$0.45 \mu\text{T}$
60 mm	$4.8 \mu\text{T}$	$1.3 \mu\text{T}$	$0.9 \mu\text{T}$	$0.48 \mu\text{T}$
70 mm	$5.5 \mu\text{T}$	$1.3 \mu\text{T}$	$0.93 \mu\text{T}$	$0.5 \mu\text{T}$

A brief summary of this study is that the magnetic field that on walls of the SSR1 cavity due to residual magnetization of the flux return is not strongly sensitive to the material choice; it is possible to configure the magnetic shielding so that the effects of residual magnetization can be neglected. **Passive shielding, if designed correctly, can properly protect the cavity from all constituents of the magnetic field generated by focusing lenses – cold or warm.**

VI. Lens with active shielding

In actively shielded magnetic systems, instead of using a flux return made of ferromagnetic material, additional superconducting winding is employed to re-direct magnetic flux. This provides a mean of controlling spatial distribution of this flux by adjusting designs of the main solenoid and the flux return winding of the lens so that the fringe field is reduced to the desired level. In this study, we will try to understand whether, by using this design approach, the requirements for the SSR1 focusing lenses can be met. As the initial configuration, a design similar to that of a focusing lens for the HWR cryomodule of PXIE [11] is considered; Fig. 13 shows schematically the design of this lens. The flux return coil is placed coaxially with the main coil. The field map of the lens installed in the HWR cryomodule (Fig. 14) shows that the magnetic field on the walls of the cavity exceeds 20 Gs, although dropping fast with the distance from the axis.

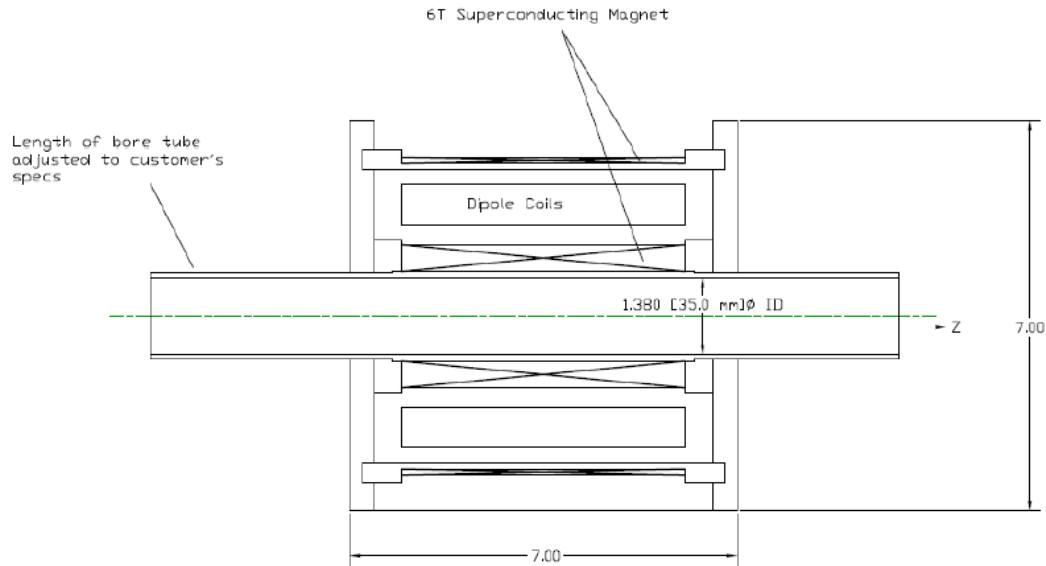


Fig 13. Active shielding scheme for a focusing lens of the HWR section of PXIE

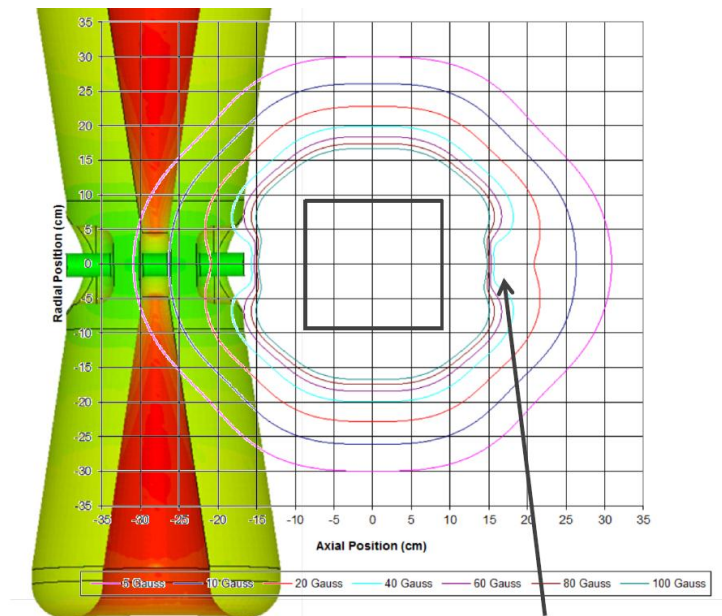


Fig. 14. Fringe field map for the SSR0 focusing lens.

To adjust the lens design for use in the SSR1 cryomodule, we need to take into account the following:

- Focusing lenses are placed on both sides of the RF cavities and generate magnetic field with opposite directions; so the Neumann boundary condition must be used in the transverse plane containing the center of the SSR1 cavity.
- The surface of the RF cavity is superconducting; so the Neumann boundary condition must be also used along the surface of the cavity.

It was possible to find a configuration that meets the main requirements for the SSR1 lens; the main parameters of this configuration are listed below:

- Round 0.35 mm NbTi strand is used to wind both coils of the lens.
- Coil length - 130 mm.
- Inner radius of the main coil – 22.5 mm.
- Outer radius of the main coil – 35.5 mm.
- Number of turns in the main coil – 11418.
- Inner radius of the flux return coil – 65 mm.
- Outer radius of the flux return coil – 67.5 mm.
- Number of turns in the flux return coil – 2283.
- Compaction factor in the windings – 0.65.
- Current - 75 A.
- Focusing strength – $4.35 \text{ T}^2\text{m}$.
- Field integral – $0.86 \text{ T}\cdot\text{m}$.

In Fig. 15 the graphs of the field distribution along walls of the cavity are shown. The maximum field on the wall of the cavity is $\sim 10 \text{ G}$ ($R = 100 \text{ mm}$). The field along the outer border of the cavity does not exceed 3 G .

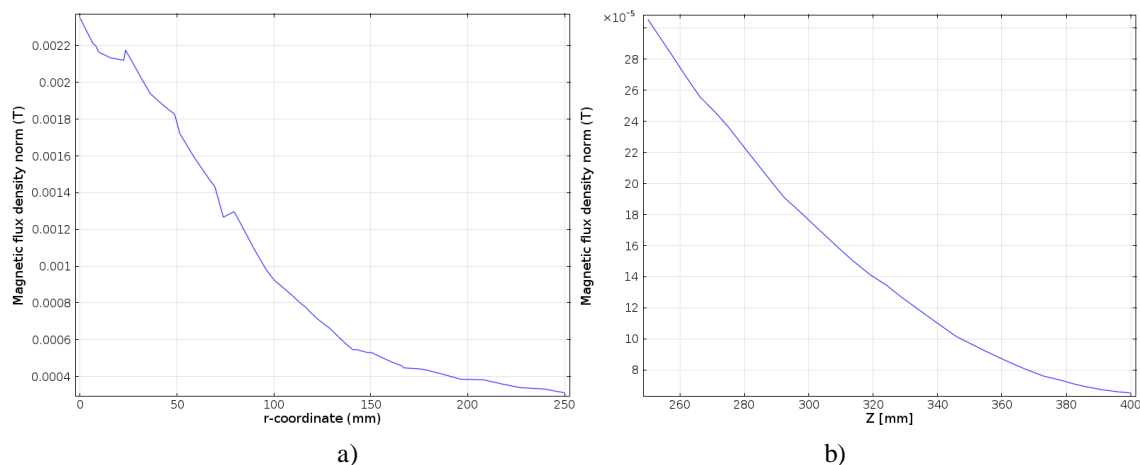


Fig. 15. Magnetic field on the cavity walls along the lines $Z = 250 \text{ mm}$ (a) and $R = 253 \text{ mm}$ (b)

Fig. 16 shows preliminary layout of this lens in the SSR1 cryomodule, and in Fig. 17 a field map with contour lines is presented. The field on wall of SSR1 cavity is expected to be lower than $\sim 10 \text{ G}$ everywhere except the central part of the outer surface of the cavity. As the fringe field requirements are marginally met, further study of the impact of the fringe magnetic field is needed to finalize the design.

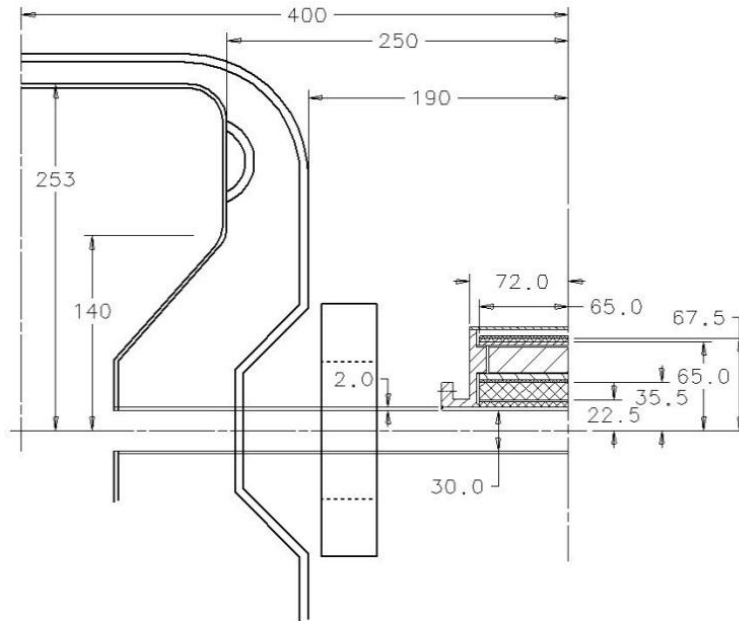


Fig. 16. Layout of the lens with active shield in the SSR1 cryomodule

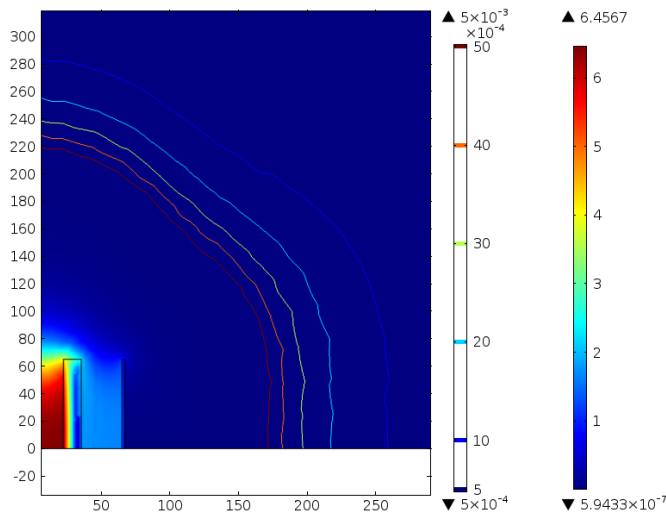


Fig. 17. Field map for the SSR1 lens with active shielding at 75 A.

IV. Conclusion

As a result several case studies, we can conclude that every design approach analyzed in this note can be considered. Each studied case has its advantages and disadvantages. The most simple (one-coil) lens design requires additional shielding efforts (though quite modest). Designs where the lens is independent of the beam pipe, while significantly reducing the risk of losing the alignment goal, do not permit direct attachment of a beam position monitor (although the option remains of integrating it into the beam pipe). Conductively-cooled systems, although attractive from the alignment point of view, require making a prototype to verify the concept. Shielding of

residuals was proved quite feasible with the use of Ni-Fe alloys designed for work at cryogenic temperature.

Actively shielded lenses can meet established requirements for fringe magnetic field without employment of ferromagnetic materials; it is more complicated in fabrication though.

Whatever lens design approach is chosen, further design studies are needed to finalize it. The issues to study include position of correctors that must be embedded in each lens and fabrication techniques that ensure needed degree of accuracy in positioning the windings.

Building and studying a prototype of a lens using a chosen approach is quite desirable to better understand lens performance in the environment of the cryomodule and be able to debug and improve the system, if needed.

References

1. Project X SSR Cryomodule Functional Requirements Specification, 10/9/2011 (see also PX doc-949-v1, Oct 26, 2011); <http://projectx-docdb.fnal.gov/>
2. J. DiMarco, et al, "Solenoid Lens Alignment in a Proton Linac at Fermilab", MT-21, Oct. 2009.
3. H. Padamsee, et al, RF Superconductivity for Accelerators, Wiley Press, 1998.
4. R.A. Laxdall, et al, "Cryogenic, Magnetic, and RF Performance of the ISAC-II Medium Beta Cryomodule at TRIUMF", PAC 2005, Knoxville, TN, USA, Proceedings, p. 2283.
5. T. Khabiboulline, et al, "Acceptable Level of Magnetic Field on the Surface of a Superconducting RF Cavity", FNAL TD note TD-12-008.
6. T. Nicol, "SSR1 Cryomodule for PXIE", doc. 1007-v1, March 6, 2012; <http://projectx-docdb.fnal.gov/>
7. G. Chlachidze, et al, HINS_SS1_SOL-02d: "Fabrication Summary and Test Results", FNAL note TD-09-001, March 2009
8. Functional Requirements Specification for a Focusing Lens of the PXIE SSR1 Cryomodule, Project X document base: doc. 1066 v.1.
9. K.-H. Mess, et al, Superconducting Accelerating Magnets, World Scientific Publishing, 1996, p. 196.
10. S. Cheban, et al, "Feasibility of Conductively-Cooled Superconducting Magnet in a Linac Cryomodule " FNAL TD note: TD-12-005, May 2012.
11. M. Kelly, Cavity String Assembly, Solenoid and Coupler for PXIE 162.5. MHz HWR Cryomodule, PXIE Review, Marh 05, 2012, <https://indico.fnal.gov/getFile.py/access?sessionId=7&resId=0&materialId=0&confId=5307>